Performance Evaluation of HSLA Steel Subjected to Underwater Explosion

R. Rajendran and K. Narasimhan

(Submitted 4 November 1999; in revised form 3 August 2000)

Performance evaluation of High Strength Low Alloy (HSLA) steel subjected to underwater explosion is of interest to materials engineers because of its structural applications in ships and submarines. Circular and rectangular plates were investigated for their explosive response because they represent panels of a ships plating. Underwater explosion bulge tests were carried out with increasing shock intensity on 4 mm thick circular plates of 290 mm diameter and rectangular plates of 300 × 250 mm to study the plastic deformation and the onset of fracture. Empirical models were developed for the prediction of depth of bulge of the plates. A fresh set of tests with various explosive charge quantities and stand offs were carried out which showed good agreement with the models. Failed edges of the plate showed slant fracture suggesting ductile mode of failure. Scanning Electron Microscopic (SEM) fractographic examination showed dimple features suggesting micro void coalescence.

Keywords explosion bulge test, plastic deformation, depth of bulge, empirical models, plate fracture, fracture analysis, terminal strain to fracture

1. Introduction

The ability of a material to withstand large plastic deformation before it fractures is a major criterion in underwater structural applications[1,2]. Air backed circular and rectangular plates clamped at their periphery simulate the panels of a ship's plating for studying the deformation and fracture behavior of hull materials[3,4]. Explosion Bulge Test (EBT) has been used as the final qualification test to verify the dynamic plasticity of structural materials. The main reason behind using explosive loading is that it promotes brittle fracture by taking advantage of the high strain rate behavior of materials[5]. Various authors have investigated the performance of steel plates and weldments subjected to explosive loading. Fox[6] observed that air backed plates clamped at their periphery fractured at their edges due to the higher differential velocity of the plate normal to itself than at any other place. Similar observation was made by Olson et al (Ref[7] and Nurick et al[8,9] in their work on air blasted mild steel plates. Hartbower et al[10,11] developed explosion bulge test as a material qualification tool for defence structural materials at Naval Research Laboratory (NRL) Washington. MIL-STD-2149 A (SH) formulated by the U.S. Navy[12] recommends air blast as the source of energy to evaluate the resistance of base materials and weldments to fracture under rapid loading conditions. Defence Research Establishment Atlantic (DREA) Canada[13,14,15] and Admiralty Research Establishment (ARE) independently developed underwater EBT to minimise the explosive charge and the environmental noise nuisance. Sumpter[16,17] developed Flawed Bulge Explosion Test (FBET) to study the propagation of dynamic cracks in fatigue pre-cracked submarine panels. Explosive testing of full thickness precracked weldments was carried out by Gifford et al[18,19] to study the fracture safety of ship structures. Johnson[20] introduced a damage number as a function of the plate velocity, total impulse acting on the plate, thickness of the plate and material damage stress. This damage number predicted the order of the magnitude of deformation for plates subjected to impact load. This damage number was specific to the size of the plate even for similar geometries. Nurick et al[21,22] extended the damage parameters for circular and rectangular plates to arrive at dimensionless parameters. These dimensionless parameters were functions of the plate geometry, total impulses, the density, and the static yield stress of the material. Johnson et al[23,24] performed underwater explosions on circular blanks with a view to improve the efficiency of explosive deformation. Cole[25] showed that for a thin plate undergoing membrane stretching, the depth of bulge is proportional to the free field impulse of the incident shock wave provided the duration of the shock pulse is much shorter compared to the diffraction time (time taken by the shock wave to travel from the edge to the centre of the plate through the shortest route and the natural period of oscillation of the plate). Remmerswaal[26] showed that explosive forming caused structural changes like mechanical twins in the metal. Explosive deformation of materials like mild steel, stainless steel and hiduminium[27] showed that the impulse per unit deflection linearly varied with the original thickness of the plate. However, empirical models for the prediction of the central deflection (depth of bulge) of plates subjected to underwater explosion was not reported in the literature.

In this investigation, underwater explosion bulge tests on High strength low Alloy (HSLA) steel plates of circular and

R. Rajendran, Naval Science and Technological Laboratory, Visakhapatnam 530 027, India; and **K. Narasimhan,** Department of Metallurgical Engineering and Materials Science, Indian Institute of Technology, Bombay 400 076, India. Contact e-mail: nara@ispat.met.iitb.ernet.in.

rectangular geometries are reported. Plate deformation and apex thickness strains were measured after each explosion. Empirical models are derived for predicting the depth of bulge of the deformed pates. A fresh set of experiments were carried out which showed good agreement with the model. Fractured plates were examined by visual inspection and by Scanning electron microscopy (SEM) to identify the mode of failure.

Table 1 Chemical composition and mechanical properties of the (High Strength Low Alloy) HSLA steel

Chemical composition (by % weight)								
Element	**C**	**Mn**	**Ni**	**Cr**	**S**	**Si**	**Cu**	**P**
Content (%)	0.12	0.7	0.9	0.8	0.035	0.6	0.5	0.035
Mechanical properties								
Yield stress (MPa)		**Ultimate tensile stress (MPa)**					**Elongation (%)**	
400				560			28	

2. Experimental Procedures

HSLA steel sheets of 6000 × 1200 × 4 mm were drawn from the Naval Dockyard, Visakhapatnam stock. The sheet was hot rolled but not heat treated. JOBIN-YVON (Cedex, France) JY50E spectrometer was used to obtain the chemical composition. A total of ten tensile tests, five in the rolling direction and five in the transverse direction were carried out at a strain rate of 0.01 s^{-1} as per ASTM E8M-89[28]. The average of the mechanical properties is taken as the representative value. The chemical composition and the mechanical properties of the HSLA steel is shown in Table 1.

Circular plates were 550 mm in diameter with an exposed area of 290 mm diameter. Rectangular plates were 550 × 450 mm with an exposed area of 300 × 250 mm. The length of the shock pulse, θ, generated during the experiments, which is given in Eq 1 below varied up to a maximum of 43 μs. This is much less when compared to the diffraction time of the plates (96.6 μs in the case of circular plates and 83 μs in the case of rectangular plates) and the natural period of oscillation of the plates (4080 μs for circular plates and 4184

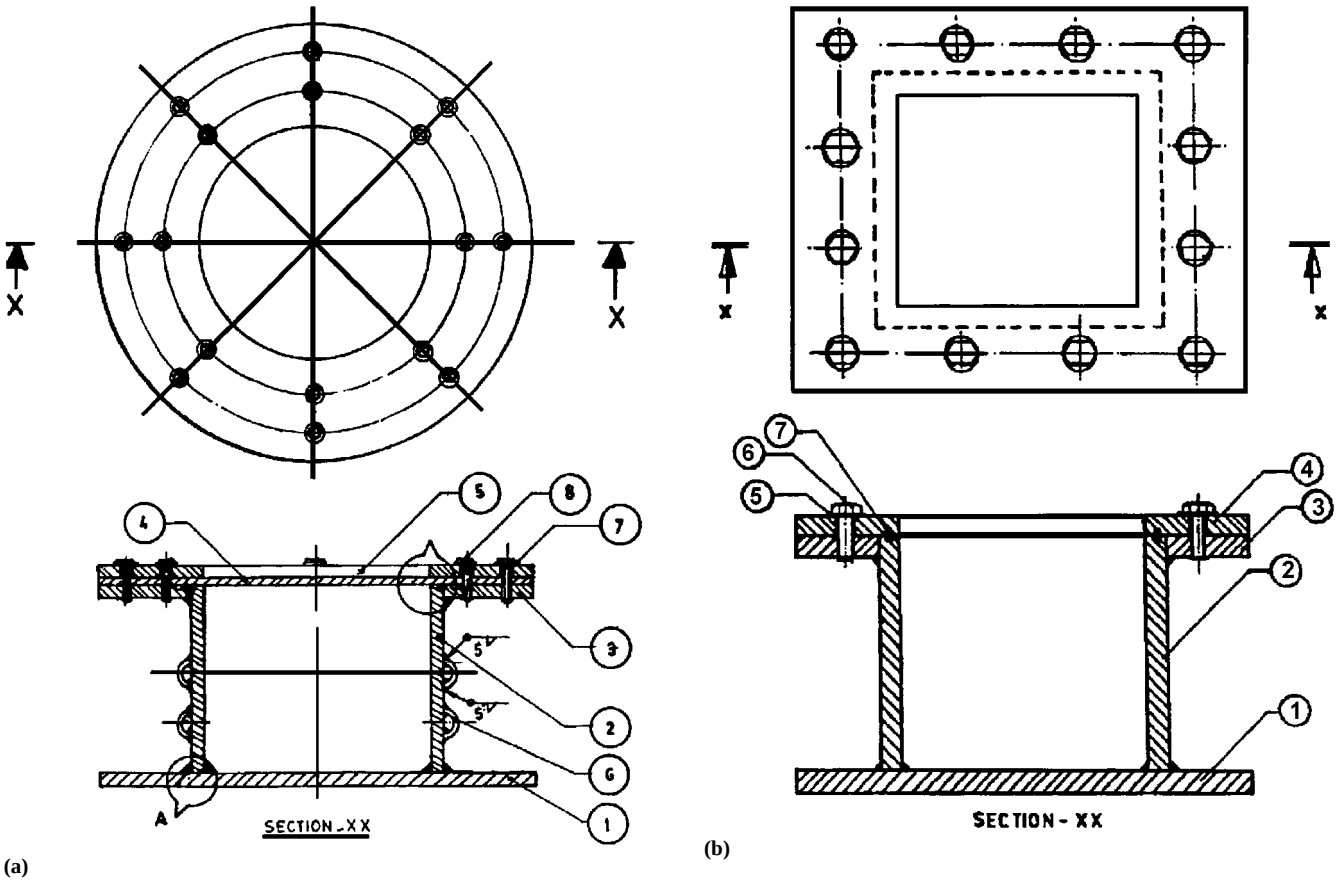

(a)

1. Bottom plate, 2. Circular drum, 3. Top plate 1, 4. Test plate, 5. Top plate 2, 6. Holding ring, 7 & 8. Bolts.

(b)

1. BOTTOM PLATE
2. RECTANGULAR BOX
3. TOP PLATE-1
4. TOP PLATE-II
5. WASHER
6. HEXAGONAL BOLT
7. RUBBER GASKET

Fig. 1 Schematic of the test assembly (**a**) for circular plates and (**b**) for rectangular plates

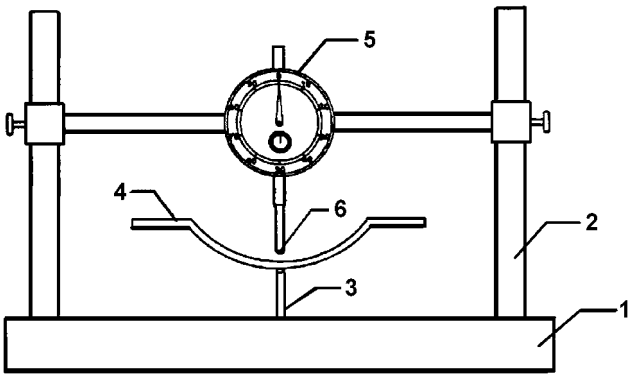

1. TABLE
2. SUPPORT COLUMN
3. SUPPORT PIN
4. TEST PLATE
5. DIAL GAUGE
6. PROBE

Fig. 2 Schematic of the dial gage setup for measuring the thickness reduction and the depth of bulge of test plates

Table 2 Summary of results of plastic deformation experiments; stand off = 15 cm

Shot No.	Explosive quantity (g)	Free field impulse (Ns/m^2)	Depth of bulge (mm)	Thinning (%)
Circular plates				
1.	5	1221	10.1	1.2
2.	10	1891	20.6	2.1
3.	15	2441	26.2	3.3
4.	20	2926	29.2	4.3
5.	30	3778	40.0	7.3
6.	40	4528	49.0	11.5
7.	50	5212	56.0	16.0
8.	60	5846	62.0	17.1
9.	70	6442	71.0	21.5
10.	80	7008	Rupture	22.3
Rectangular plates				
1.	5	1221	12	1.25
2.	10	1891	23	2.50
3.	15	2441	27	3.75
4.	20	2926	32	4.75
5.	30	3778	42	6.25
6.	40	4528	50	7.25
7.	50	5212	58	12.50
8.	60	5846	65	16.25
9.	70	6442	72	21.25
10.	80	7008	Rupture	22.5

μs for rectangular plates). Therefore, the depth of bulge was proportional to the free field impulse of the shock wave[25].

$$\theta = 100.6(W^{1/3})\left(\frac{W^{1/3}}{S}\right)^{-0.22} \mu s \qquad \text{(Eq 1)}$$

where W is the quantity of explosive charge in kg and S is the stand off in m.

The explosive used was having the energy content of 1240 kcal/kg. The chemical composition was 91% by weight

(a)

(b)

Fig. 3 A photographic view of the circular and rectangular plates deformed during underwater explosion: (**a**) circular plate, explosive charge quantity = 60 g of PEK-1; and (**b**) rectangular plate, explosive charge quantity = 40 g of PEK-1

$C_3H_6N_6O_6$ and 9% wax. The product molecules of the explosives were CO, CO_2, H_2O, NO, CH_4 and H_2 as gases and carbon as solid. The explosive had a density of 1600 kg/m^3, melting temperature of 473K and detonation velocity of 8380 m/s. The detonation of the explosive was initiated by an electric detonator. The detonator had a tetryl ($C_7H_5O_8N_5$) base explosive, followed by a sensitive mercury fulminate in a cap and was initiated by passing a current of 0.9 ampheres through a hot wire. The explosion products undergo a series of expansion and compression along with migration in the vertical direction underwater and eventually vent out at the surface of the water. Since all the explosions were non-contact in nature (that is there was definite distance between the test plate and the explosive), there was no possibility for the explosive products to come into contact with the plate. The explosive after detonation becomes a hot incandescent mass that instantly compresses the water around it to make a spherical shock front. The spherical shock wave becomes a plane wave after travelling for some distance. The pressure of the combustion products is around 5000 MPa and the temperature is around 3000K.

A schematic of the assemblies used for the experiments is shown in Fig. 1. The explosive was weighed, shaped in to a

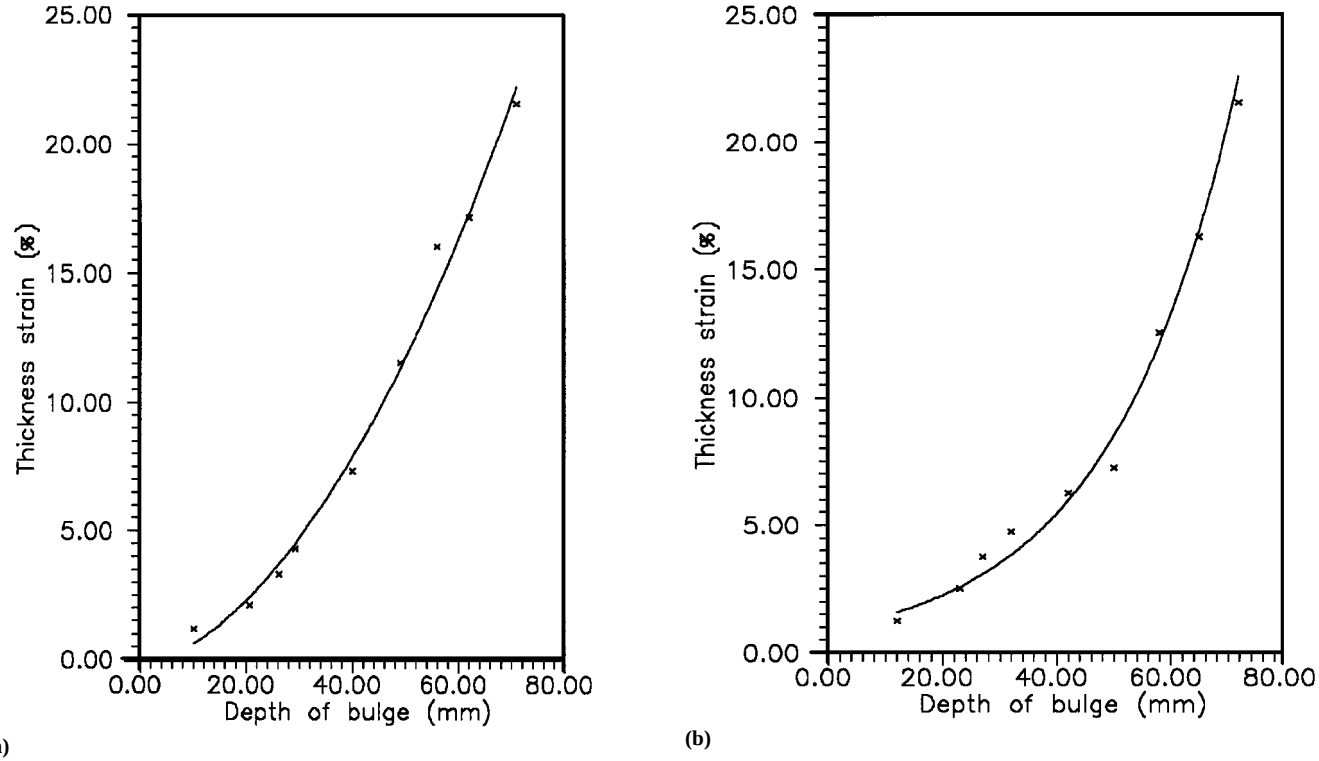

Fig. 4 Variation of thickness strain as a function of apex bulge depth: (**a**) for circular plates and (**b**) for rectangular plates

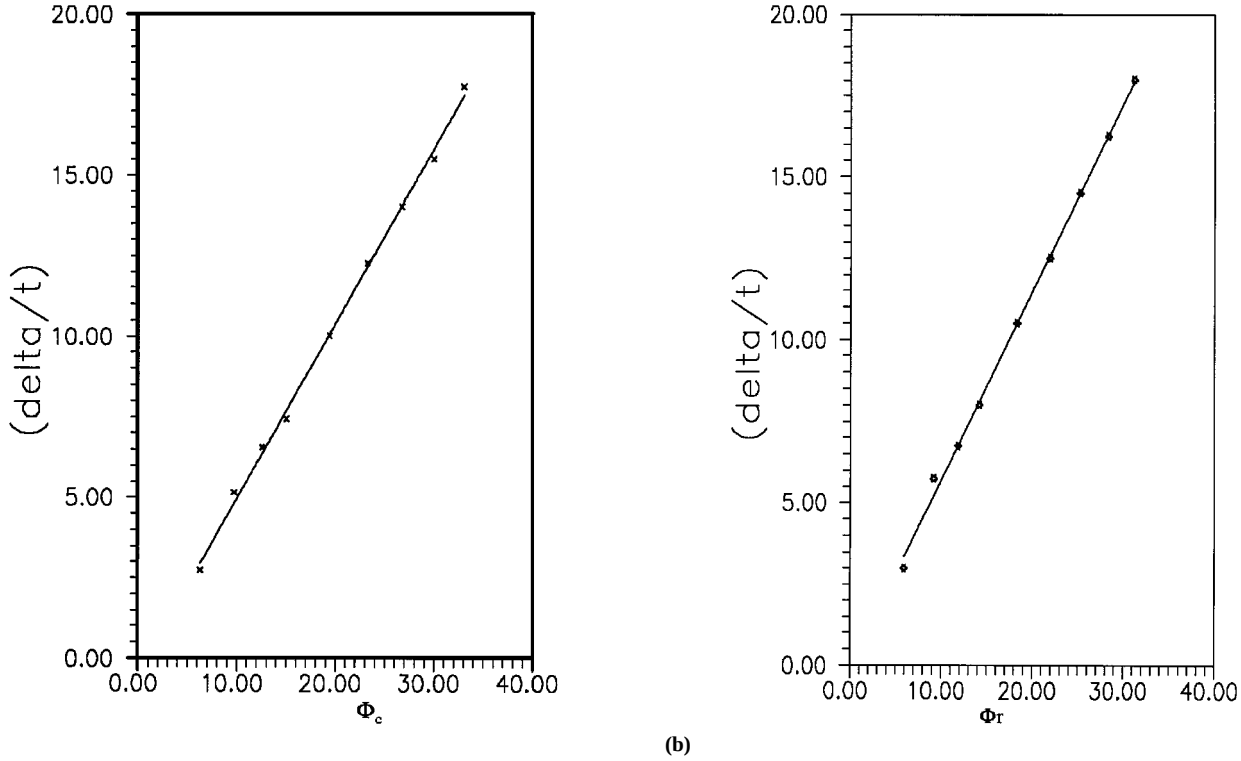

Fig. 5 Variation of deflection-thickness ratio as a function of dimensionless parameter: (**a**) for circular plates and (**b**) for rectangular plates

cylinder, inserted in to a plastic container and positioned from the explosive charge holder at the required stand with the center of explosive coinciding with the center of the test plate. The electric detonator was then inserted in to the explosive with a firing cable leading to a firing circuit. The whole setup was immersed in to a shock tank (15 × 12 × 10 m) to a depth of

Table 3 Chemical composition and mechanical properties of commercial mild steel

Chemical composition (by % weight)					
Element	**C**	**Mn**	**S**	**Si**	**P**
Content (%)	0.15	0.85	0.017	0.25	0.018
Mechanical properties					
Yield stress (Mpa)		**Ultimate tensile stress (MPa)**		**Elongation (%)**	
320		470		28	

Table 4 Chemical composition and mechanical properties of Tisten 55 steel

Chemical composition					
Element	**C**	**Mn**	**S**	**Si**	**P**
Content (%)	0.2	1.7	0.04	0.4	0.04
Mechanical properties					
Yield stress (Mpa)		**Ultimate tensile stress (MPa)**		**Elongation (%)**	
410		540		20	

2 metres. The assembly was taken out of the shock tank after each explosion and the plate was dismantled for measuring the depth of bulge and the apex thickness strain.

A dial gauge arrangement (with a accuracy of 0.01 mm) was fixed with the existing MTS 886-361 A shock testing system as shown in Fig. 2 for measuring the thickness reduction of the plates undergoing plastic deformation. Fractured specimens were examined visually for finding the macroscopic mode of failure. Samples were prepared for Scanning Electron Microscopic (SEM) examination using JEOL T330A machine.

3. Results and Discussion

The results of underwater explosion bulge test are shown in Table 2. The thickness reduction for circular plates varied from 1.2% to 21.5%. For rectangular plates, it was 1.25 to 21.5%. The depth of bulge varied from 10.1 to 71 mm for circular plates and 12 mm to 72 mm for rectangular plates. A photographic view of the test plates deformed during underwater explosion is shown in Fig. 3. The variation of thickness strain as a function of deflection at the apex of the plate is shown in Fig. 4.

3.1 Empirical Prediction

The following dimensionless numbers that were proposed by Nurick[21,22] for air blasted plates take into account the total impulse, I_t, acting on the plate.

$$\Phi_c = \frac{I_t}{\pi R t^2 (\rho_p \sigma_y)^{1/2}} \pi R^2 \qquad \text{(Eq 2)}$$

for circular plate and

Table 5 Summary of validation results in comparison with empirical prediction

(a) Circular plates

Shot No.	Explosive quantity (g)	Stand off (cm)	Φ_c	δ_{em} (mm)	δ_{ex} (mm)
1.	30	20	15.00	31.0	29.2
2.	40	20	17.98	37.4	37.2
3.	50	20	20.70	40.3	41.0
4.	60	20	23.20	46.1	48.6
5.	50	30	14.42	31.0	29.2
6.	50	40	11.17	22.7	21.6
7.	50	50	9.16	15.6	18.3
8.	60	40	12.52	24.3	25.6
9.	60	50	10.27	19.2	20.7

(b) Rectangular plates

Shot No.	Explosive quantity (g)	Stand off (cm)	Φ_r	δ_{em} (mm)	δ_{ex} (mm)
1.	70	50	10.68	27.3	26.6
2.	70	40	13.03	33.1	31.8
3.	70	30	16.84	41.7	40.2
4.	60	50	9.69	27.0	24.4
5.	60	40	11.82	33.1	29.2
6.	60	30	15.28	38.7	36.8
7.	50	50	8.64	24.0	22.1
8.	50	40	10.54	29.3	26.3
9.	50	30	13.62	35.2	33.1

Φ_r: Dimensionless parameter; δ_{ex}: Experimental deflection; δ_{em}: Empirical deflection.

$$\Phi_r = \frac{I_t}{2t^2 (ab\rho_p \sigma_y)^{1/2}} ab \qquad \text{(Eq 3)}$$

for rectangular plate. In the above equations, Φ_c is the dimensionless parameter for the circular plate, Φ_r is the dimensionless parameter for the rectangular plate, t is the original thickness of the plate, ρ_p is the mass densiy and σ_y is the static yield stress of the plate material, R is the radius of the circular plate and a and b are the sides of the rectangular plate.

However, in underwater explosion, the total impulse acting on the plate is not easily derivable since there are incident, reflected and rarefaction components which modify the incident pressure pulse both in magnitude and direction[29]. Therefore the dimensionless numbers given in Eq 3 and 4 are modified as a function of free field impulse, I_f, (that is the impulse of the incident shock pulse per unit area) acting on the plate:

$$\Phi_c = \frac{I_f}{\pi R t^2 (\rho_p \sigma_y)^{1/2}} \pi R^2 \qquad \text{(Eq 4)}$$

for circular plate and

$$\Phi_r = \frac{I_f}{2t^2 (ab\rho_p \sigma_y)^{1/2}} ab \qquad \text{(Eq 5)}$$

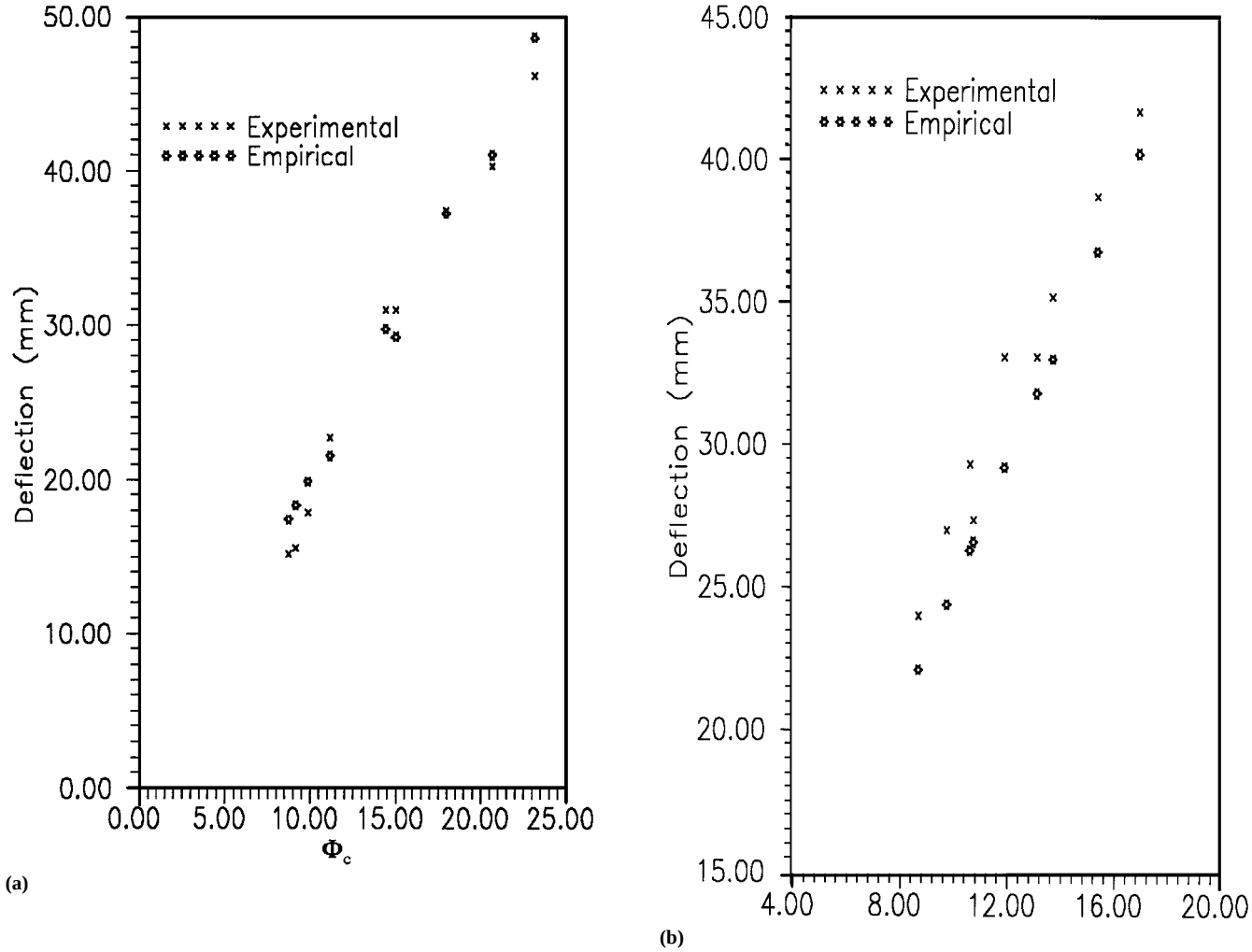

Fig. 6 Comparison of deflection of the plate with empirical model: (**a**) circular plates and (**b**) rectangular plates

Table 6. Summary of validation experiment results on commercial mild steel and Tisten 55 steel rectangular plates

Shot No.	Material	Thickness (mm)	Explosive quantity (g)	Stand off (cm)	Φ_r	δ_{em}	δ_{ex}
1.	Mild steel	2	60	50	43.28	49.5	47.1
2.	Mild steel	4	50	15	28.23	65	65
3.	Mild steel	4	60	15	31.66	71	71
4.	Tisten 55 steel	8	60	30	3.73	22.4	21.1

Φ_r: Dimensionless parameter; δ_{ex}: Experimental deflection; δ_{em}: Empirical deflection.

for rectangular plate. The free field impulse I_f in Eq 4 and 5 is given as

$$I_f = 6359 \frac{W^{0.63}}{S^{0.89}} \quad \text{(Eq 6)}$$

where: W is the TNT equivalent of the explosive change expressed in kilograms, S is the stand off distance in meters.

Graphical representation of the deflection-thickness ratio as a function of the dimensionless parameter Φ is shown in Fig. 5. Linear curve fitting is made to the data since the deflection is proportional to the impulse of the plate[17,25]. The deflection-thickness ratio is experimentally found to be

$$\left(\frac{\delta}{t}\right)_c = 0.541\Phi_c - 0.433 \quad \text{(Eq 7)}$$

for circular plates and

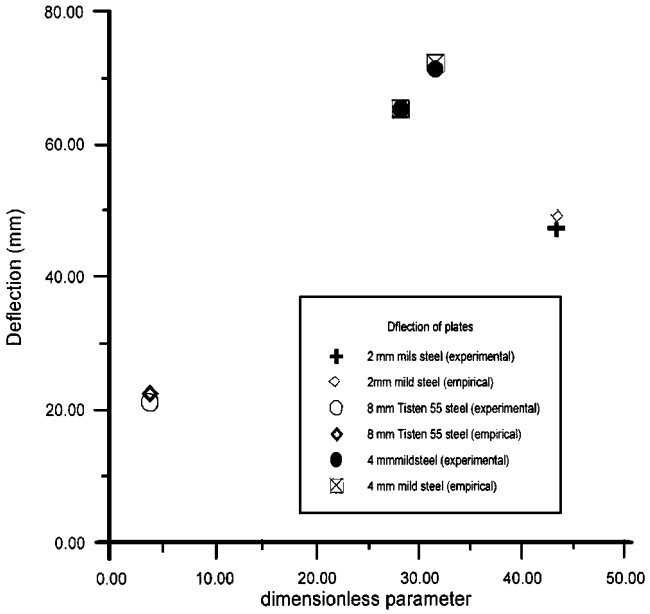

Fig. 7 Variation of central deflection of commercial mild steel and Tisten 55 steel rectangular plates as a function of the dimensionless parameter Φ_r

$$\left(\frac{\delta}{t}\right) = 0.553\Phi_r + 0.741 \qquad \text{(Eq 8)}$$

for rectangular plates.

From the above models, once the explosive quantity, stand off, test plate dimensions and material properties are known the depth of bulge is readily obtained.

3.2 Model Validation

In order to see the applicability of the empirical model, a separate set of experiments were carried out on the circular and rectangular plates with different explosive charge quantities and stand offs. Experiments were also carried out on commercial mild steel rectangular sheets of 2 mm and 4 mm (whose chemical composition and mechanical properties are given in Table 3) and a Tisten 55 steel (made by Tata Iron and Steel Corporation, Jamshedpur, India) rectangular plate (whose chemical composition and mechanical properties are given in Table 4). The results of the validation experiments on the HSLA steel plates are summarized in Table 5. The explosive quantity was varied from 30 to 60 grams and the stand off was varied from 20 cm to 50 cm. The variation of the central deflection of the HSLA steel plate and its comparison with the empirical models is shown in Fig. 6. The results of the commercial mild steel and Tisten 55 rectangular plates is shown in Table 6. The explosive charge quantity was varied from 50 to 60 grams and the stand off was varied from 15 cm to 50 cm. The variation of central defletion of mild steel and Tisten 55 plates and its comparison with the empirical model is shown in Fig. 7. The agreement of the central deflection data with the empirical prediction was 85 to 99.5% for the HSLA, 94% for Tisten 55 steel and 94 to 100% for commercial mild steel. This shows that the empirical model has an excellent prediction over a wide range of explosive quantities and stand offs and for different materials.

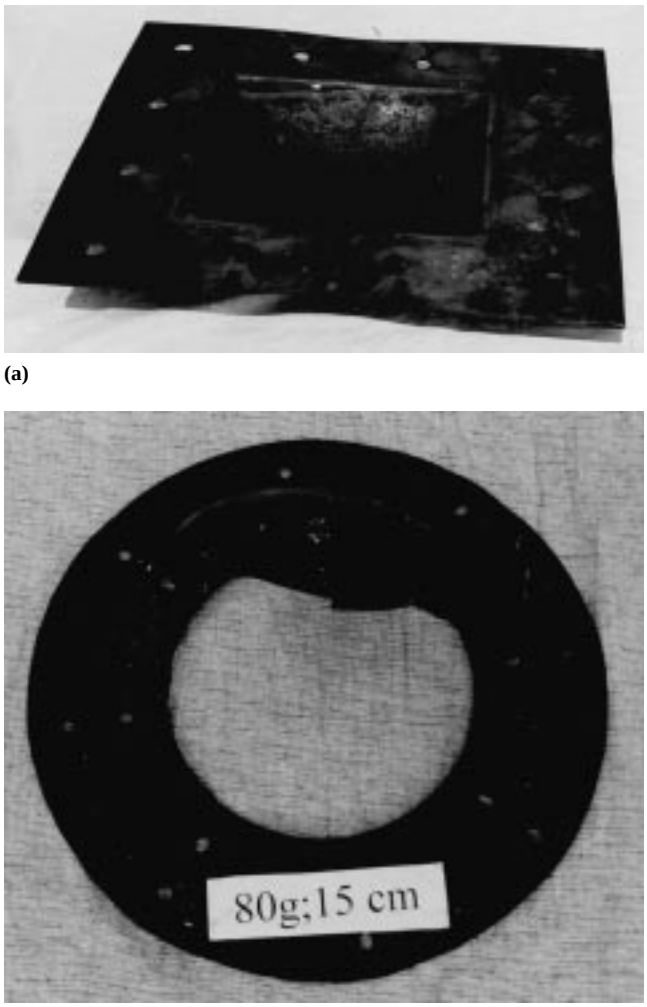

(a)

(b)

Fig. 8 Photographic view of the: (**a**) fractured rectangular and (**b**) fractured circular plates

3.3 Fracture Analysis

A photographic view of the circular and rectangular plates fractured at their edges is shown in Fig. 8. The plate fractured all around its edge. A closer view of the failed edge is shown in Fig. 9. From Fig. 9, it was observed that the failure of the plate was slant fracture across the thickness of the plate, which was typical of ductile failure[30]. Ductile failure is desired from ship designers' point of view since it absorbs an enormous amount of shock energy before the ship hull tears apart and loses its structural integrity. Also, this observation dispels the common notion that shock fracture is always brittle in nature. The factors which influence the brittle fracture are[17] temperature, material stress level, structural thickness, fabrication practice, defect occurance and strain rate. The effect of test temperature on the mode of fracture is out of the scope of this investigation. The fractured surface was brownish yellow in color, suggesting heavy oxidation due to the heat generated by

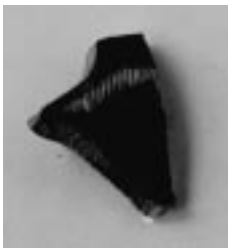

(a)

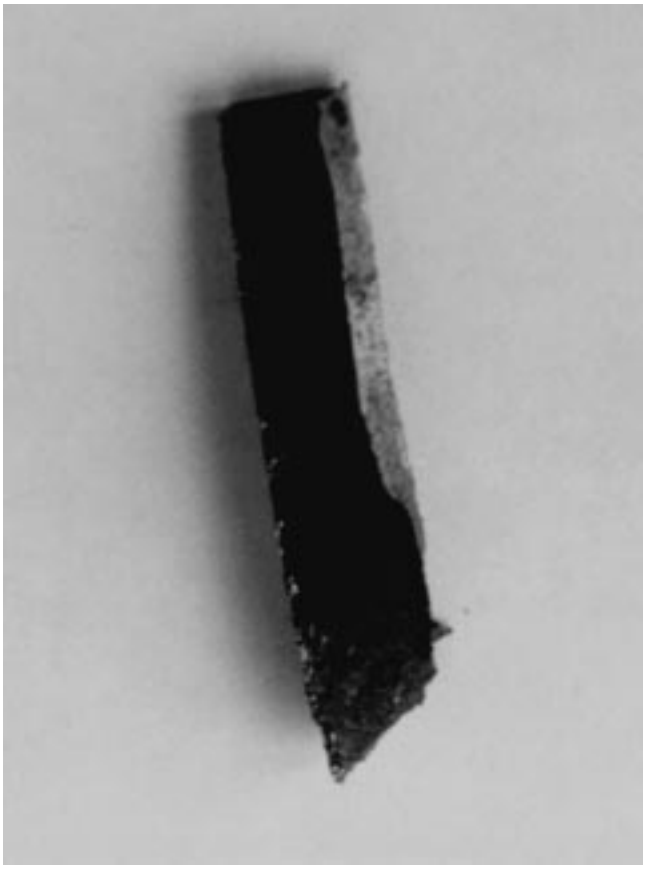

(b)

Fig. 9 A close view of the fractured edges. A 45° slant is observed across the thickness indicating ductile failure: (**a**) fractured sample of the rectangular plate and (**b**) fractured sample of the circular plate

dynamic plastic deformation. Typically, the strain rate experienced during underwater explosive deformation goes up to $600s^{-1}$[31]. However, there is no chance of the explosive products coming in contact with the fractured surface. Scanning Electron Microscopic (SEM) fractography of the failed sample is shown in Fig. 10. Dimple features show that the fracture was by microvoid coalescence.

The fracture strain at the apex of the plate was 22.3% for circular plates and 22.5% for rectangular plates. A comparison of thickness strain for circular and rectangular plates show that the terminal strain to fracture is a material parameter and hence is independent of geometry.

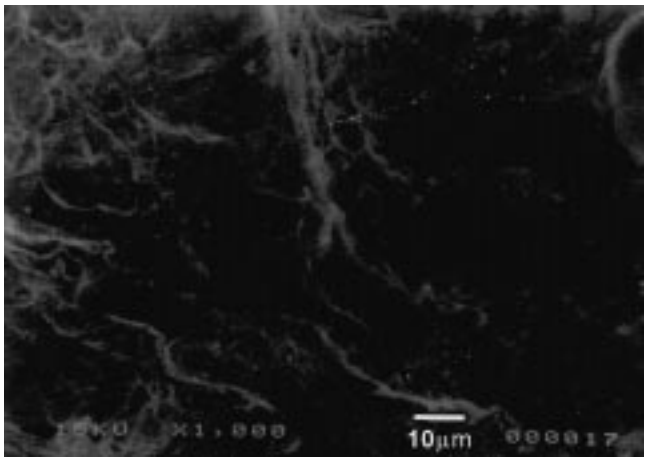

(a)

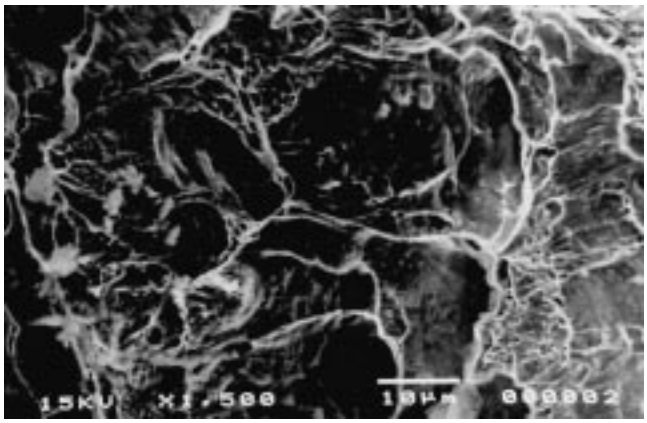

(b)

Fig. 10 SEM fractography of the failed plates: (**a**) circular plate and (**b**) rectangular plate

4. Conclusions

Dynamic deformation and fracture evaluation of 4 mm HSLA steel plates subjected to underwater explosion was carried out for circular and rectangular geometries and the point of rupture was identified to be along the edges where the plates were clamped to the test assembly.

Empirical models were developed for the prediction of depth of bulge of the circular and rectangular plates. Fresh experiments conducted with various stand offs and explosive charge quantities showed that the experimental data were in good agreement with the models. Experiments were also carried out on commercial mild steel of two thicknesses and Tisten 55 steel which showed encouraging comparison with the empirical prediction.

Both circular and rectangular plates fractured at their edges exhibiting browinsh yellow surface due to heavy oxidation. The failure of the plate was by slant fracture across the thickness of the plate, which is tyical of ductile failure. The Scanning Electron Microscopic (SEM) examination of the fractured surfaces showed dimple features suggesting crack propagation by micro void coalescence.

A comparison of thickness strain for circular and rectangular

plates shows that the terminal strain to fracture is a material parameter and, hence, independent of the plate geometry.

References

1. J.D.G. Sumpter: in *Advances in Marine Structures*, C.S. Smith and J.D. Clarke, eds., Elsevier Applied Science Publishers, New York, NY, 1986, pp. 326-46.
2. J.D.G. Sumpter: *J. Naval Sci.*, 1987, vol. 13 (4), pp. 258-70.
3. A.H. Keil: *Introduction to Underwater Explosion, Underwater Explosion Research Division*, Norfolk Naval Shipyard, Portsmouth, VA, 1956, p. 104.
4. A.H. Keil: *Trans. Soc. Naval Architects Marine Eng.*, 1961, vol. 69, pp. 366-410.
5. J. Ahmad, K. Wong, and J.F. Porter: *60th Shock and Vibration Symp.*, 1989, vol. 1, pp. 137-71.
6. E.N. Fox: *Compendium of Underwater Explosions Res.*, 1947, vol. 1, pp. 1-83.
7. M.D. Olson, G.N. Nurick, and J.R. Fagnan: *Int. J. Impact Eng.*, 1993, vol. 3 (2), pp. 279-91.
8. G.N. Nurick and G.C. Shave: *Int. J. Impact Eng.*, 1996, vol. 8 (1), pp. 99-116.
9. G.N. Nurick, M.E. Gelman, and N.S. Marshall: *Int. J. Impact Eng.*, 1996, vol. 18 (7–8), pp. 803-27.
10. C.E. Hartbower and W.S. Pellini: *Welding J.*, 1951, Oct., pp. 499s-511s.
11. C.E. Hartbower and W.S. Pellini: *Welding J.*, 1951, June, pp. 307s-318s.
12. U.S. Navy: *Standard Procedure for Explosion Bulge Testing of Ferrous and Non-ferrous Metallic Materials and Weldments*, MIL-STD-2149a (sh), 1990.
13. J.F. Porter: *Response of SMA and Narrow Gap HY80 Weldments to Explosive Shock*, Technical Memorandum 88/206, DREA, Nova Scotia, Canada 1988.
14. J.F. Porter and J. Ahmad: *61*st Shock and Vibration Bull., 1992, vol. 4, pp. 101-11.
15. J.F. Porter and D.O. Morehouse: *Can. Fracture Conf.*, Halifax, NS, Canada, 1990.
16. J.D.G. Sumpter: *Prediction of Critical Crack Size in Plastically Strained Weld Panels*, ASTM-STP-995, ASTM, Philadelphia, PA, 1989, pp. 415-32.
17. J.D.G. Sumpter: *Advances in Marine Structures-2*, C.S. Smith and R.S. Dow, eds., Elsevier Applied Science Publishers, New York, NY, 1991,
18. L.N. Gifford and J.W. Dally: in *Advances in Marine Structures-2*, C.S. Smith and R.S. Row, eds., Elsevier Applied Science Publishers, New York, NY, 1991, pp. 23-41.
19. L.N. Gifford, J.R. Carlberg, A.J. Wiggs, and J.B. Sickle: in *Fracture Mechanics 21st Symp.*, ASTM-STP-1074, J.P. Gudas, J.A. Joyce, and E.M. Hucket, eds., ASTM, Philadelphia, PA, 1990, pp. 157-77.
20. W. Johnson: *Impact Strength of Maerials*, Edward Arnold, London, 1972.
21. G.N. Nurick and J.B. Martin: *Int. J. Impact Eng.*, 1989, vol. 8 (2), pp. 171-86.
22. G.N. Nurick: *Int. Conf. on Mechanical Properties of Materials at High Rates of Strain*, Institute of Physics Society, Oxford, United Kingdom, No. 12, Sess. 9, 1989.
23. W. Johnson, A. Poyton, H. Singh, and F.W. Travis: *Int. J. Mech. Sci.*, 1966, vol. 8, pp. 237-70.
24. W. Johnson, K. Kormi, and F.W. Travis: *Int. J. Mech. Sci.*, 1966, vol. 6, pp. 287-301.
25. R.H. Cole: *Underwater Explosion*, Princeton University Press, Princeton, NJ, 1948, pp. 414-18.
26. J.R. Remmerswaal: *The Peaceful Use of Explosives*, Sheet Metal Industries, 1962, pp. 475-86.
27. T.M. Finnie: *Explosive Forming of Circular Diaphragms*, Sheet Metal Industries, 1962, pp. 391-98.
28. *Standard Test Methods for Tension Testing of Metallic Materials*, ASTM E8M-89, ASTM, Philadelphia, PA, pp. 147-61.
29. A.H. Kennard: *Compendium of Underwater Explosions Research, Office of Naval Resarch*, Washington, DC, 1944, vol. 3, pp. 11-64.
30. R.W. Hertzberg: *Deformation and Fracture Mechanics of Engineering Materials*, 3rd ed., John Wiley & Sons Inc., New York, NY, 1989, pp. 250-51.
31. T. Bednarsky: *Int. J. Mech. Sci.*, 1969, vol. 1, pp. 949-59.